Arch. Metall. Mater. **63** (2018), 1, 393-401

DOI: 10.24425/118953

M. KUKURYK*#

THE ANALYSIS OF DEFORMATION AND FORECASTING MICROSTRUCTURE IN THE FORGING PROCESS OF THE X6CrNiTi18-10 AUSTENITIC STEEL

The paper presents the analysis of the three-dimensional strain state for the cogging process of a forging (type: shaft) of the X6CrNiTi18-10 austenitic steel with the application of the finite element method. The results of the thermal-mechanical simulation of the hot cogging process on flat and shaped anvils, taking under consideration boundary conditions applied in industrial practice, are presented. In the research, a new method of forging, consisting in the introduction of the initial forging of the stock on anvils which have convex work surfaces, and further forging on shaped anvils, was applied. The results of the calculations make it possible to determine effective strain distribution, effective stress, mean stresses and temperature in the volume of a forging. The solution was supplemented by the addition of the model of microstructure development in the course of deformation. The conducted research constitutes the basis for determining the best possible technological process of the initial forging of a cast ingot, and provide the possibility of forecasting the deformations and parameters of the microstructure.

Keywords: hot forging, austenitic steel, FEM, microstructure

1. Introduction

The objective of the contemporary technologies of forging is to obtain forgings which represent a very high quality, and that means products which have the required shape and dimensional tolerance, and also to obtain the properties and the structure of a material which will be the best possible one in the aspect of the intended application and the functional characteristics of a detail [1]. Perfecting the construction of machines and devices, which are more and more frequently required to function in a reliable and a failure-free, frequently makes it necessary that construction materials making it possible to work at elevated temperatures and resistant to the corrosive effect of the environment are applied. Among those materials, a significant group is constituted by austenitic stainless steels, the composition of which is based upon nickel and chromium [2]. A significant problem for stainless steels is that of intercrystalline corrosion, which destroys the cohesion of crystallites, reaches substantially deeply, and is difficult to be noticed. To meet the objective of improving intercrystalline corrosion resistance, small quantities of titanium were added to the X6CrNiTi18-10 steel for the purpose of bonding carbon. A similar result may be achieved by means of the application of niobium as an alloy-forming element [3].

The issue of the deformability of austenitic stainless steels is significant in the thermal-mechanical forming processes of forgings which have an elongated shape, and it ought to be borne in mind that the process of the forging of steels which have the high contents of nickel and chromium is, to a significant degree, limited by the low level of their plastic properties, and by rapid hardening [4,5]. From the technological point of view, what is particularly significant, is the state of deformation and stress in the axial zone of the material being forged, determined, first and foremost, by the shape of tools, and also by the presumed technological parameters [6,7]. The natural heterogeneousness of the structure, and the defects of a stock, and also the heterogeneousness of deformations, resulting from the process of forging, contribute as the consequence of that to the different final properties of products. In this situation, the modification of the technology of the forging of the X6CrNiTi18-10 steel by means of plastic deformations ought to be conducted with the application of selected shaped anvils, and the best possible technological parameters [8,9]. The shape and the size of crystallites may be changed within a wide scope in the functions of the shape of a tool, strain, strain rate, and also temperature, and this way, exert influence upon the properties of forgings. The mathematical modelling of the development of microstructure and the final mechanical properties of steels is a supporting tool which has been applied more and more frequently over the recent years [10,11].

Taking the determinants referred to above under consideration, the thermal-mechanical and microstructural simulation of the cogging process on flat and shaped anvils was conducted, and the changing conditions of deformation were taken under

* CZĘSTOCHOWA UNIVERSITY OF TECHNOLOGY, FACULTY OF MECHANICAL ENGINEERING AND COMPUTER SCIENCE, 42-200 CZĘSTOCHOWA, 21 ARMII KRAJOWEJ AV., POLAND

Corresponding author: kukurykm@itm.pcz.pl

consideration. That course of action makes it possible to improve the quality of elongated rods made of austenitic steel, and provides the possibility of forecasting internal quality. The paper does not present the detailed technological process. Only selected, the most interesting results describing the material being investigated, considering final forming operations.

2. Thermal-mechanical model

For the modelling of three-dimensional plastic metal flow in the course of the cogging process of the X6CrNiTi18-10 steel, the computer program DEFORM-3D, consisting of the mechanical, thermal and microstructural part, was taken advantage of. The detailed description of that program is presented in the work [12]. The solution was sought with the application of the finite element method, combined with solving Fourier equation for non-stationary heat flows. The details of this approach are given in [13].

To meet the objective of the assessment of the conditions of heat flow on the surface of contact between a forging and anvils, the value of exchanged thermal flux was determined, taking under consideration press pressure (100 MPa) and surface coarseness (R_a = 3.5 μm). The research encompassed registering temperatures at a few selected internal points of a forging and on the surface of anvils, taking advantage of the sheathed thermocouples of the K-type. The precision of the measurement of temperature amounted to ±10 K. To determine the values of thermal flux exchanged on the surface of contact, numerical investigations were conducted, with the introduction of boundary conditions being acquired by means of experiments. The value of the thermal flux set on the surface of contact between a forging and anvils was determined with the application of the minimum norm error condition, which was determined as the sum of squares of differences in measured temperatures, and those calculated with the application of the finite element method. Similar methodology was applied for the purpose of determining thermal flux acquired from the surface of random forging by the surrounding milieu.

3. Equations for describing dynamic recrystallization

For the purpose of developing the equations of the model of microstructure evolution, the relationships described by Johnson-Mehl-Avrami-Kolmogorov (JMAK) [14-16] were applied. The equation describing critical strain of dynamic recrystallization ε_c, was replaced with the equation for peak strain ε_p in the flow stress curve, by which the initial grain size d_0 and strain rate $\dot{\varepsilon}$ are both taken under consideration. Deformation in the case of maximum stress (peak value) was determined with the application of the following relationship:

$$\varepsilon_c = a_0\,\varepsilon_p, \text{ where } \varepsilon_p = a_1\,d_0^{\,n_1}\,\dot{\varepsilon}^{m_1}\exp\frac{Q_1}{RT} + c_1 \qquad (1)$$

The Avrami equation is used to describe the relationship between the dynamic recrystallization fraction X_{DRX} and the effective strain ε:

$$X_{DRX} = 1 - \exp\left[-\beta_d\left(\frac{\varepsilon - a_o\varepsilon_p}{\varepsilon_{0,5}}\right)^{k_d}\right] \qquad (2)$$

in which $\varepsilon_{0.5}$ denotes the strain for 50% recrystallization:

$$\varepsilon_{0,5} = a_2\,d_0^{\,h_2}\,\varepsilon^{n_2}\,\dot{\varepsilon}^{m_2}\exp\frac{Q_2}{RT} + c_2 \qquad (3)$$

The recrystallized grain size is expressed as a function of initial grain size, strain, strain rate and temperature:

$$d_{DRX} = a_3\,d_0^{\,h_3}\,\varepsilon^{n_3}\,\dot{\varepsilon}^{m_3}\exp\frac{Q_3}{RT} + c_3 \qquad (4)$$

The average grain size was determined with the application of the following relationship:

$$d_{ave} = X_{DRX}\,d_{DRX} + (1 - X_{DRX})\,d_0 \qquad (5)$$

The nomenclature of the above formulation is: ε_p is the peak strain in the flow stress curve, a_o is a constant with the value of 0.8, d_o is the initial grain size (μm), Q_1 is the activation energy of deformation (kJ/mol), R is the universal gas constant with the value of 8.31 J mol^{-1} K^{-1}, T is the absolute temperature (K), β_d is the Avrami material constant with the value of 0.693, ε is the true strain, $\dot{\varepsilon}$ is effective strain rate, k_d is the Avrami exponent with a commonly reported value of 2, $\varepsilon_{0.5}$ is the strain of 50% DRX, Q_2 is the activation energy for recrystallization (kJ/mol), Q_3 is the activation energy (kJ/mol), d_{ave} is the average grain size (μm), $a_1, n_1, m_1, c_1, a_2, h_2, n_2, m_2, c_2, a_3, h_3, n_3, m$ *and* c_3 are constants, based on the computational results from the experimental data for the X6CrNiTi18-10 austenitic steel.

The effects of deformation temperature and strain rate on the deformation behaviors can be represented by Zener-Hollomon parameter (Z) in an exponential equation:

$$Z = \dot{\varepsilon}\exp\left(\frac{Q}{RT}\right) \text{ where } \dot{\varepsilon} = A\left[\sinh(\alpha\sigma_p)\right]^n \exp\left(\frac{-Q}{RT}\right) \qquad (6)$$

where Q is the activation energy of hot deformation, R is the universal gas constant, T is the absolute temperature, α, A, n are the material constants. As the result of deriving the log ithm of equation (6), the following relationship was obtained:

$$\ln A + n\ln\left[\sinh(\alpha\sigma_p)\right] - \frac{Q}{RT} - \ln\dot{\varepsilon} = 0 \qquad (7)$$

Upon the basis of it, the activation energy of the process of plastic deformation was determined, and so were the parameters of equation (6) with the application of the graphical method. The measurements encompassed the range of temperatures: 1023-1373 K and the scope of strain rate: 0.25-5.5 s^{-1}, with the application of repeating every trial three times. The graphical relationships $\ln(\sigma_p) = f(T^{-1})$, and also $\ln(\sigma_p) = f(\ln\dot{\varepsilon})$, which respectively for constant strain rate $\dot{\varepsilon}$ and constant temperature T constitute the straight line making it possible to determine

activation energy with the application of the following relationship:

$$Q = nR\frac{\partial(\ln\sigma_p)}{\partial(1/T)}\Big|_{\dot{\varepsilon}=const.} \text{ where } n = \frac{\partial(\ln\dot{\varepsilon})}{\partial(\ln\sigma_p)}\Big|_{T=const.} \quad (8)$$

The determined values of coefficients for the austenitic steel being analysed appearing in the formulas (1) – (4) amounted to:

$$a_0 = 0.83,\ a_1 = 0.0035,\ n_1 = 0.30,\ m_1 = 0.0190,$$
$$c_1 = 0.39,\ Q_1 = 53500,\ \beta_d = 0.693,\ a_2 = 0.058,$$
$$h_2 = 0.35,\ m_2 = 0.080,\ n_2 = 0.88,\ Q_2 = 35500,$$
$$c_2 = 0.090,\ a_3 = 1409,\ h_3 = 0.80,\ n_3 = 0.89,$$
$$m_3 = -0.124,\ Q_3 = -54535,\ c_3 = -0.125,\ d_0 = 100\,\mu\text{m}.$$

4. Results and discussion

The values of true stress for the X6CrNiTi18-10 austenitic steel were presumed upon the basis of conducted plastometric investigations for the different values of strain, strain rate and for the determined scope of the temperature of hot plastic working ($\sigma_p = \sigma(\varepsilon, \dot{\varepsilon}, T)$). The research encompassed the compression of axial-symmetrical samples, which have the following dimensions: ø30 × 30 mm on a cam plastometer (type: MAEKAWA-Japan). The conditions of friction on the surface of contact were maintained at the level similar to that observed in the case of conditions dominating in the course of making cogging process. The samples were deformed within the following scope of temperatures 1123 K-1423 K, for the following scope of true strain: 0.105-0.693 and for the following scope of strain rate: 0.25-5.5 s^{-1}.

The example course of relationship between true stress and strain and temperature for two selected strain rates: 1.5 s^{-1} and 2.8 s^{-1}, and also for three temperature values: 1123 K, 1223 K and 1473 K, are shown in Figure 1. The determined curves $\sigma_p = f(\varepsilon)$ manifest the typical maximum of true stress, which occurs in the case of true strain amounting to, approximately, 0.50 and it ought to be borne in mind that the location of that maximum is not dependent upon temperature.

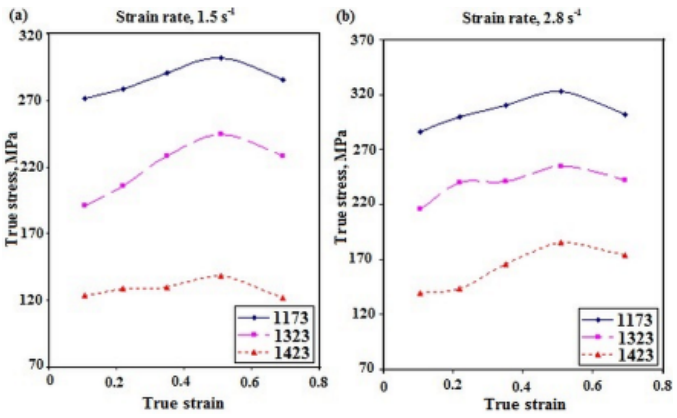

Fig. 1. True stress-strain curves for the X6CrNiTi18-10 austenitic steel at various temperatures with strain rate of (a) 1.5 s^{-1} and (b) 2.8 s^{-1}

In numerical calculations and in experimental model testing, it was presumed that the diameter of the charge would be ø80 mm × 200 mm, and that it would be made of the X6CrNiTi18-10 steel, which has the following chemical composition: C-0.10%, Mn-2%, Cr-18%, Ni-9.0%, Si-0.80% and Ti-0.65. It was presumed that the initial temperature of the stock would be 1373 K, and that of anvils 523 K (those are the values of heating them up in industrial conditions). The cogging process was conducted in flat anvils, angular convex anvils, oblique anvils and radial-rhombic anvils with an impression angle of 135° × 135°, as shown in Figure 2. Cogging process on flat anvils was conducted with the application of the traditional method (comparative basis), whereas on oblique anvils, and also on the radial-rhombic anvils with an impression angle of 135° × 135°, two-stage forging was applied. In the initial phase of forging, the initial charge was first preforged on the angular convex anvils with an angle of 135°. The final deformation was conducted on shaped anvils in four passes divided by turning of the ingot by 90°, and maintaining the constant value of actual strain ε_h = 0.35 and the constant relative feed amounting to l_w = 0.75 in every pass.

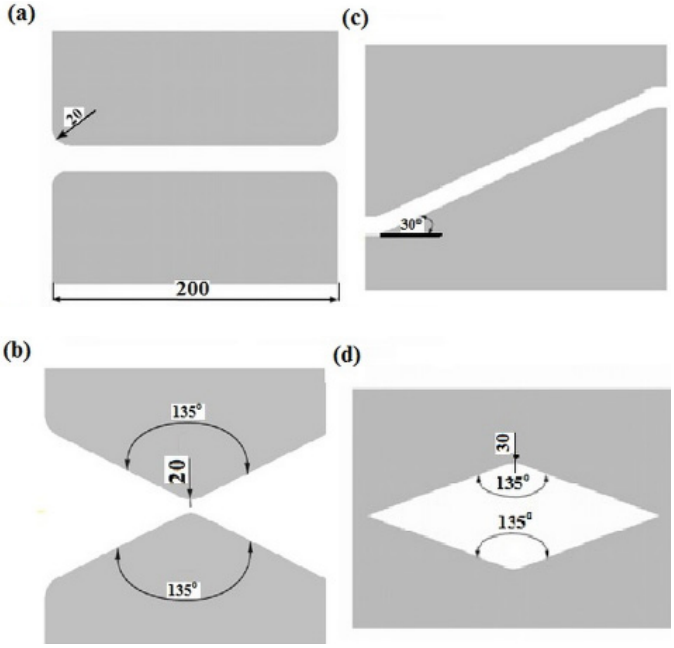

Fig. 2. Shape of anvils: (a) flat, (b) angular convex, (c) oblique, (d) radial-rhombic

For the austenitic steel being researched, and also for the material applied in the X37CrMoV51 anvils, the profile of properties such as: density, specific heat and thermal conduction was presumed upon the basis of experimental data, and set as temperature functions. The relationship between density and temperature for the steel being researched was determined by means of experiment and approximated with the application of the following relationship:

$$\rho = -1\cdot10^{-13}T^5 + 5\cdot10^{-10}T^4 - 5\cdot10^{-7}T^3 + -1\cdot10^{-4}T^2 - 0.0104T + 7800 \quad (9)$$

In the case of the elongation of a material which has a round cross-section on flat anvils (Fig. 3a), the non-uniformity of the deformations was comparatively high. In the presented distribution of local deformations after the fourth pass (ε_h = 1.40), it is possible to distinguish several typical zones. The area adjacent to the surfaces of anvils underwent small deformations ($\varepsilon_i/\varepsilon_h$ = 0.77-0.96). The largest deformation occurred in the central part of a forging, whereas the values of the effective strain ε_i significantly exceeded the value of true strain ε_h($\varepsilon_i/\varepsilon_h$ = 1.75), and the edge zones of a forging were the area of indirect deformations ($\varepsilon_i/\varepsilon_h$ = 0.96-1.16). That part of the forging material may be subjected to the impact of tensile stresses for the part of not deformed external zones, and also strongly deformed center (Fig. 3c). The process of forging was accompanied by a stable temperature distribution in the central part of a forging caused by heat emission in connection with plastic deformation, and the contact of hot metal with cool tools caused a reduction in temperature by ΔT = 90-120° (Fig. 3d). The substantial non-uniformity of deformation distribution in cogging process on flat anvils is responsible for the fact that obtaining forgings which have high internal quality is significantly more difficult than ensuring the required shape and geometry of a forging.

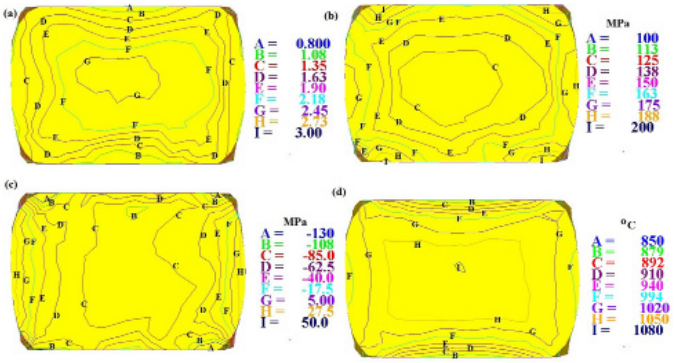

Fig. 3. Distribution of effective strain (a), effective stress (b), mean stress (c) and temperature (d) on the cross-section of the specimen X6CrNiTi18-10 steel during the cogging process in flat anvils after fourth pass

Forging practice is based upon the most versatile flat anvils, in which the forging of a high-alloy, low plasticity steels causes particularly adverse consequences. For that very reason, improved flat anvils, which have oblique work surfaces, making it possible to perform the complete technological process without the time-consuming replacement of tools, were applied in this work. It is shown by the course of changes to the effective strain ε_i in the center of deformation gap in the function of the true strain ε_h (Fig. 4a) and relative feed l_w (Fig. 4b) on oblique anvils that it is possible to exert a deliberate influence upon the local values of the effective strain in the certain zones of a forging, while simultaneously maintaining the expedient values of the state of stress indicators k_σ (the proportion of mean stress σ_m to the effective stress σ_i) for the technologies of forging. Simultaneously with increase in the true strain, the values of the effective strain in the central part of the deformation gap increase significantly; it ought to be borne in mind that the state of stress indicator more and more expedient values, and dangerous tensile stress in the central part of a forging disappears and is converted into compressive stresses.

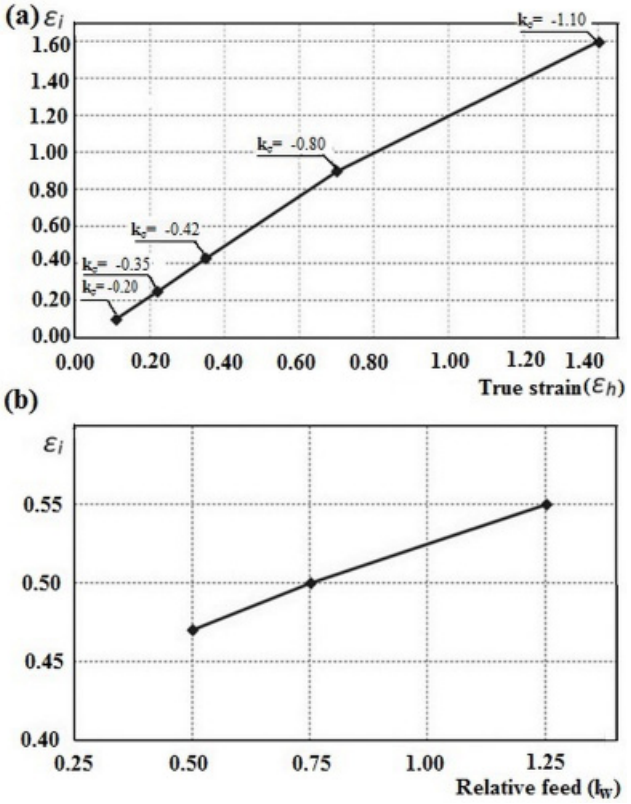

Fig. 4. Influence of true strain (a) and relative feed (b) on the effective strain after the cogging process of the specimen X6CrNiTi18-10 steel in the oblique anvils ((a) l_w = 0.75; (b) ε_h = 0.70)

In the presented the effective strain distribution, after the fourth pass (ε_h = 1.40) it is possible to ascertain that the applied oblique anvils manifested an expedient influence upon deformation distribution and stresses in the process of the forging of the X6CrNiTi18-10 austenitic steel (Fig. 5). A very expedient, similar to uniform, the effective strain distribution on the surface of the cross-section of a forging ($\varepsilon_i/\varepsilon_h$ = 2.01-2.04 – Fig. 5a) was obtained. A similar one was the effective stress distribution presented in Figure 5b (101-125 MPa). The major advantage of forging on those anvils is the comparatively expedient state of stress in the central part of a forging (Fig. 5c). Only a small part of the material situated in the corners of a forging may be subjected to the impact of tensile stresses. The process of forging on those anvils was accompanied by a stable temperature distribution in the central part of a forging caused by the heat emission of plastic deformation, and the contact of hot metal with cool tools caused decrease in temperature in the vicinity of the surfaces of contact by ΔT = 70-100°C (Fig. 5d). The measurements of the temperature of the surface of a forging after deformation with the application of a thermovision camera evidenced the compatibility of the temperature of it, and the calculated temperature alike (differences amounted to ±10°C).

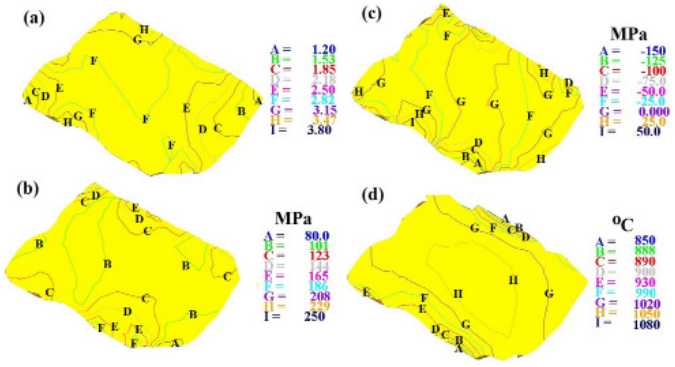

Fig. 5. Distribution of effective strain (a), effective stress (b), mean stress (c) and temperature (d) on the cross-section of the specimen X6CrNiTi18-10 steel during the cogging process in the oblique anvils after fourth pass

Figure 6 represents the distribution of effective strain and mean stress after deformation of the X6CrNiTi18-10 austenitic steel in angular convex anvils with an angle of 135° after the first and the second deformations (after aligning the concavity in the flat anvils). The true strain is the same for the first and second reductions ($\varepsilon_h = 0.35$). The anvils used in the preforging showed a favourable effect on the strain and mean stresses distributions in the forging process. The greatest effective strain values occurred in the workpiece areas situated under the convex anvil surfaces ($\varepsilon_i = 0.69$ – after the first deformation, $\varepsilon_i = 0.96$ after the second deformation). A great advantage of forging in these anvils is a relatively high uniformity of effective strain distribution after the second deformation (Fig. 6b). For the angular convex anvils with an angle of 135°, no tensile stresses were found to occur in the axial zone of the workpiece. The presented distribution of mean stress (Fig. 6B) indicates a possibility of tensile stresses occurring only in a very small area in the side zones of the workpiece.

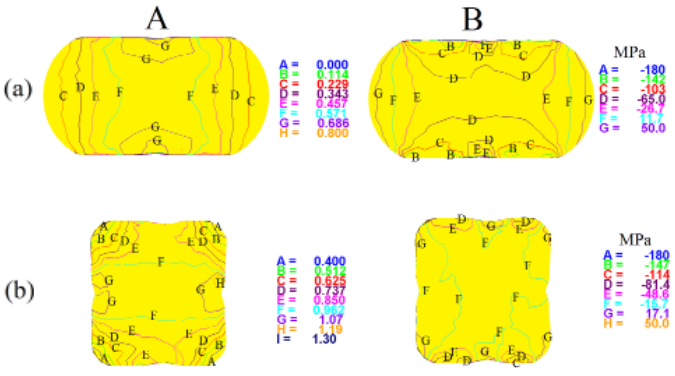

Fig. 6. Distribution of effective strain (A) and mean stress (B) on the cross-section of the specimens X6CrNiTi18-10 steel during the cogging process in angular convex anvils with an angle of 135° after the first reduction (a) and the second reduction (b). True strain $\varepsilon_h = 0.35$

In Figure 7, the effective strain distribution, the effective stress, mean stresses and temperature after the fourth pass ($\varepsilon_h = 1.40$) in radial-rhombic anvils with an impression angle of 135° × 135°, is presented. On the major part of a cross-section, a very expedient, similar to uniform, the effective strain distribution ($\varepsilon_i/\varepsilon_h = 2.66$) was obtained, which exerted an expedient influence upon the preforging of the axial zone of a forging (Fig. 7a). It was solely in the corners ($\varepsilon_i/\varepsilon_h = 2.85$-$3.21$), and also in lateral side zones of a forging that deviations in the effective strain distribution ($\varepsilon_i/\varepsilon_h = 1.45$-$1.75$) were obtained. A similar one is the effective stress distribution presented in Figure 7b (115-143 MPa). For those anvils, the occurrence of tensile stresses in the axial zone of a forging was not ascertained. The presented mean stress distribution (Fig. 7c) evidences the possibility of the occurrence of tensile stresses only on a very small area situated in the lateral zones of a forging. The process of forging was accompanied by a stable temperature distribution on the major part of the section of a forging caused by the heat emission of plastic deformation and the work of friction forces (Fig. 7d).

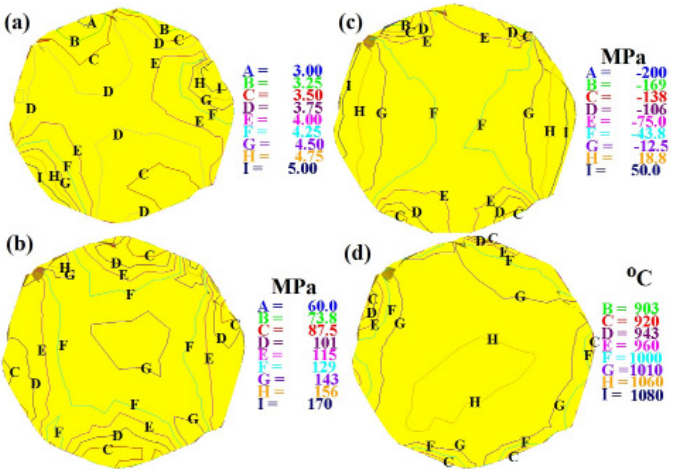

Fig. 7. Distribution of effective strain (a), effective stress (b), mean stress (c) and temperature (d) on the cross-section of the specimen X6CrNiTi18-10 steel during the cogging process in radial-rhombic anvils with an impression angle of $\alpha = 135° \times 135°$ after fourth pass

The distribution of the dynamically recrystallized volume fraction, and also the average grain size distribution on the surface of the cross-section of samples after the fourth pass, deformed on flat anvils, is presented in Figure 8. The dynamically recrystallized volume fraction reached its maximum in the centre of a forging, and amounted to 0.750-0.875. The smallest average grain size was obtained for the central area of a forging, and it amounted to 25.0-40.0 μm. On the surface of contact of deformed metal and anvils, and also on the lateral surfaces of a forging, the significantly larger average grain sizes were obtained (73.0-80.0 μm).

The distribution of the dynamically recrystallized volume fraction, and also the average grain size distribution on the surface of the cross-section of samples after the fourth pass, deformed on oblique anvils, is presented in Figure 9. The dynamically recrystallized volume fraction reached, on the major part of the cross-section, the value of 0.875 (Fig. 9a). The smallest the average grain size was obtained for the central part of a forging, and it amounted to 28.8 μm. On the lateral surfaces of a forging, larger average grain sizes (41.3-47.5 μm) were obtained.

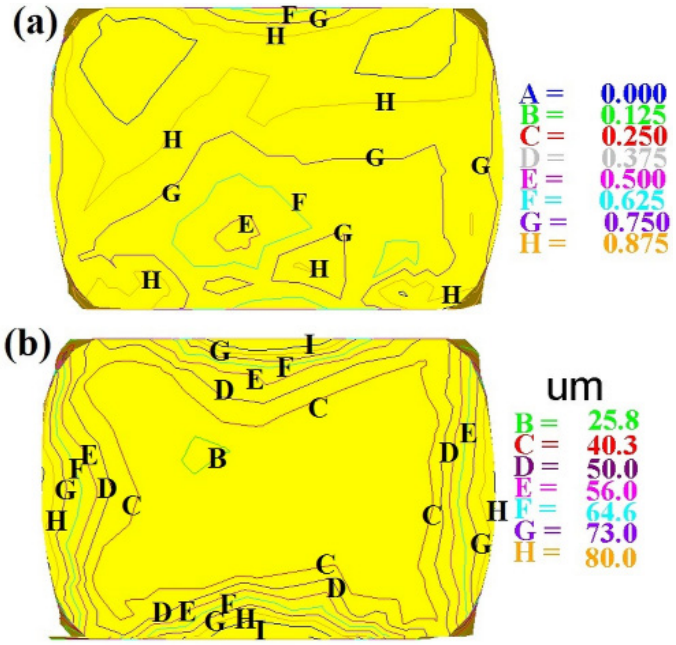

Fig. 8. Distribution of the dynamically recrystallized volume fraction (a) and mean grain size (b) on the cross-section of the specimens X6CrNiTi18-10 steel during the cogging process in flat anvils after fourth pass

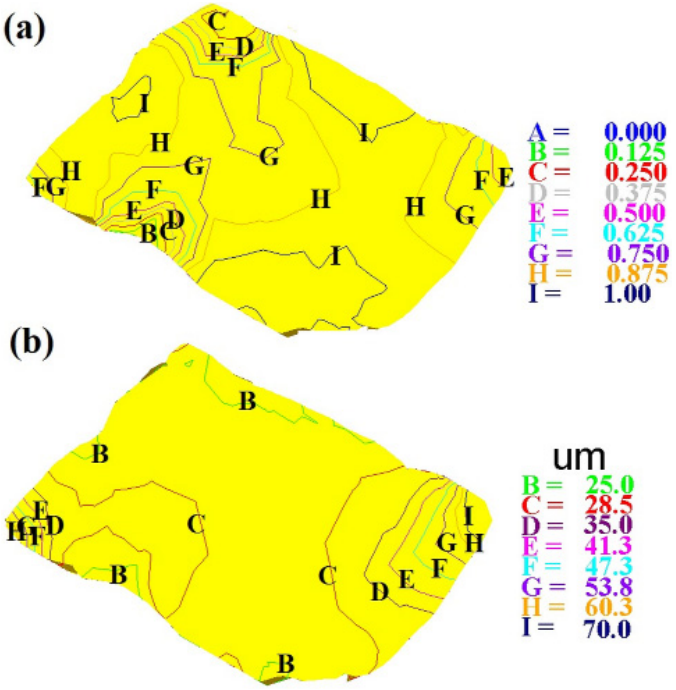

Fig. 9. Distribution of the dynamically recrystallized volume fraction (a) and mean grain size (b) on the cross-section of the specimens X6CrNiTi18-10 steel during the cogging process in the oblique anvils after fourth pass

The distribution of the dynamically recrystallized volume fraction, and also the average grain size distribution on the surface of the cross-section of samples after the fourth pass, deformed in radial-rhombic anvils with an impression angle of 135° × 135°, is presented in Figure 10. The microstructure which was obtained was to a large extent recrystallised and homogeneous on the most part of the specimen cross-section (Fig. 10a). The average grain size distribution on the surface of the cross-section of the sample was more uniform in comparison with distribution on oblique anvils. The intensive preforging of the axial zone of a forging was conducive to the formation in this area of fine-grained structure, which amounted to 17.5-20.0 μm (Fig. 10b). As the result of the initial preforging on convex anvils, and also multi-operational forging with ingot turning in the remaining areas of a forging, an expedient microstructure (the average grain size amounted to 15-17.5 μm) was obtained. The conducted comparative analysis gives rise to the conclusion that the greatest effect of crystallite disintegration and the high uniformity of the distribution of it was obtained on radial – rhombic anvils with an impression angle of 135° × 135°. On flat anvils, the largest average grain sizes, and also the greatest non-uniformity of the distribution of them, was obtained.

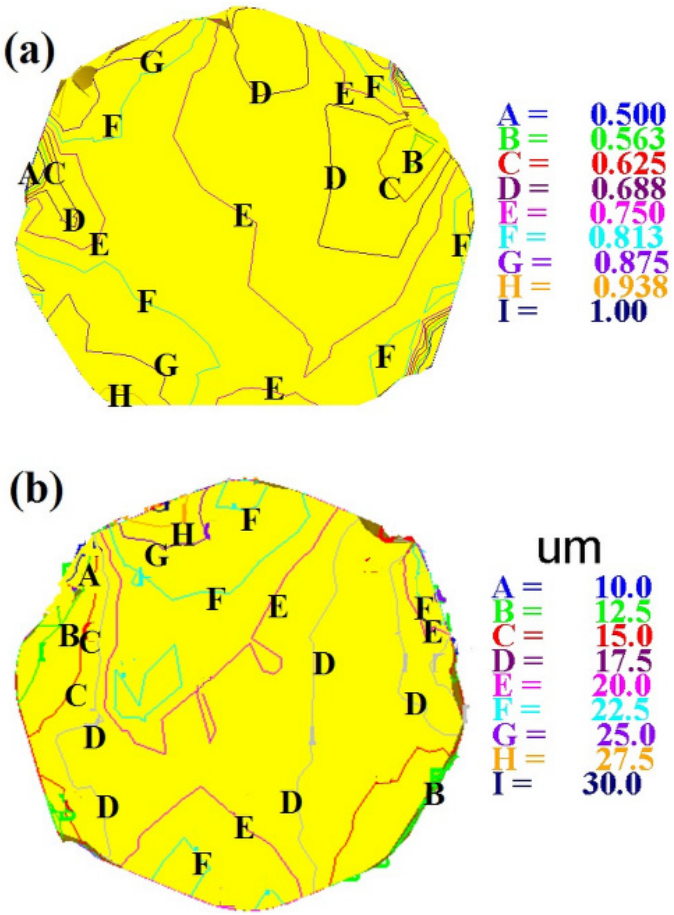

Fig. 10. Distribution of the dynamically recrystallized volume fraction (a) and mean grain size (b) on the cross-section of the specimens X6CrNiTi18-10 steel during the cogging process in radial-rhombic anvils with an impression angle of α = 135° x 135° after fourth pass

For the purpose of confirming the results of model testing, the numerical calculations of and experimental research into the cogging process of a cast ingot of the X6CrNiTi18-10 austenitic steel on flat anvils in industrial conditions were conducted. Output data for the thermal-mechanical simulation of cogging pro-

cess were acquired from the programme of the forging of a cast ingot the mass of which amounts to 8000 kg on an integrated forging line, equipped with a 20 MN press with two manipulators and controlled by a computer. The thermal-mechanical model of the process of forging in industrial conditions was taking under consideration the profile of a forging press, the kind of material, the temperature of heating up, time of transport from the furnace to the press, time of setting subsequent crumples and the temperature of tools, the conditions of friction on a surface of contact, the coefficient of charge emission, and also conductivity coefficients. It was presumed that a cast ingot had the body which after equalizing convergences had the following dimensions: ø800 × 1250 mm. The initial temperature of a material was presumed to be at the level of 1373 K (in accordance with the industrial plan of forging), whereas the initial temperature for anvils at the level of 523 K. Forging was conducted on flat anvils in 12 passes with ingot turning by the angle of 90°, while simultaneously maintaining the following values of true strain: $\varepsilon_h = 0.105$ (pass 1 – 4), $\varepsilon_h = 0.162$ (pass 5 – 8) and $\varepsilon_h = 0.356$ (pass 9-12). In particular technological passes, the constant value of relative feed, amounting to $l_w = 0.75$, was applied. The initial grain size was presumed to amount to $d_0 = 240$ µm. In the course of experimental forging, after every pass, the temperature of a deformed material was recorded with the application of an installed thermovision camera.

The results of the model testing were compared with the selected results of industrial research after the eighth technological pass because the stock materials were subjected to that same degree of preforging (the forging ratio of 2.25). The analysis of the fields of deformations and stresses evidenced the qualitative and quantitative similarity between the changes to the effective strain, mean stresses and the parameters of microstructure (Fig. 11). The largest deformations were occurring in the central part of a forging ($\varepsilon_i = 2.48$-2.70, Fig. 11a). The area adjacent to the surfaces of anvils underwent significantly smaller deformations ($\varepsilon_i = 1.05$-1.33), the edge zones of a forging were the area where deformations were indirect ($\varepsilon_i = 1.33$-1.60). That part of the material of a forging may be subjected to the impact of tensile stresses for the part of non-deformed external zones, and also

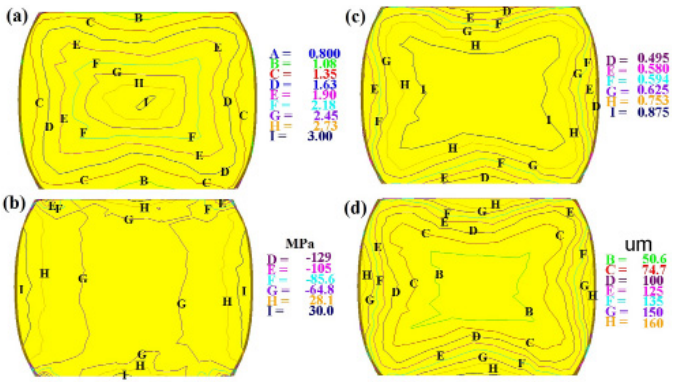

Fig. 11. Distribution of effective strain (a), mean stress (b), the dynamically recrystallized volume fraction (c) and mean grain size (d) on the cross-section of the specimen X6CrNiTi18-10 steel during the cogging process in flat anvils after the eighth pass (forging ratio of 2.25)

the strongly-deformed center (Fig. 11b). After the eighth pass, the dynamically-recrystallized volume fraction was amounting to 0.750-0.875 (Fig. 11c). The smallest grain size was obtained for the central area of a forging, and the value of it amounted to 50.0-75.0 µm. On the surface of contact between the deformed metal and the anvils, and also on the lateral surfaces of a forging, significantly larger grain sizes (150.0-160.0 µm) were obtained (Fig. 11d).

The presented selected results of research after 12 pass (the forging ratio of 4.0 – Fig. 12) confirmed the occurrence of significant qualitative and quantitative changes to the effective strain distributions, mean stresses and the parameters of microstructure, simultaneously with increase in the forging ratio. The largest deformations in the central part of a forging increased their size nearly three times, and amounted to $\varepsilon_i = 6.38$-7.19 (Fig. 12a). The area adjacent to the surfaces of anvils underwent deformations which were three times larger as well ($\varepsilon_i = 2.31$-4.75), and a similar increase in the value of deformations was observed to occur in the edge zones of a forging. The lateral parts of a forging can still be subjected to the impact of tensile stresses (Fig. 12b). As the result of the application of the process of multi-stage forging, with the application of interoperational ingot turning, the process of dynamic recrystallization encompassed nearly complete volume of the plastic zone, and the dynamically-recrystallized volume fraction was amounting to 0.875-1.00 (Fig. 12c). On the major part of the surface of the cross-section of a forging, the average grain size amounted to 23.8 µm (Fig. 12d). It was only on the surface of contact between the deformed metal and the anvils, and also on the lateral surfaces of a forging that the larger average grain sizes (37.5-51.3 µm) were obtained.

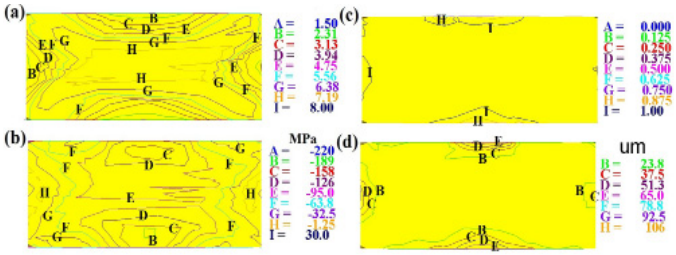

Fig. 12. Distribution of effective strain (a), mean stress (b), the dynamically recrystallized volume fraction (c) and mean grain size (d) on the cross-section of the specimen X6CrNiTi18-10 steel during the cogging process in flat anvils after the twelfth pass (forging ratio of 4.0)

The calculated temperature after particular passes was contrasted with the experimental measurement of temperature in the course of the programmed forging of steel cast ingots, the mass of which amounted to 8000 kg, in an integrated forging line (Fig. 13). The cogging process on flat anvils in industrial conditions was accompanied by a stable temperature in the central part of a forging, and the contact of hot metal with cool tools brought about the formation of the significant gradients of temperature in the vicinity of the surface of contacts. That natural gradient of temperature was conducive to intensive the preforging of the axial zone of a forging.

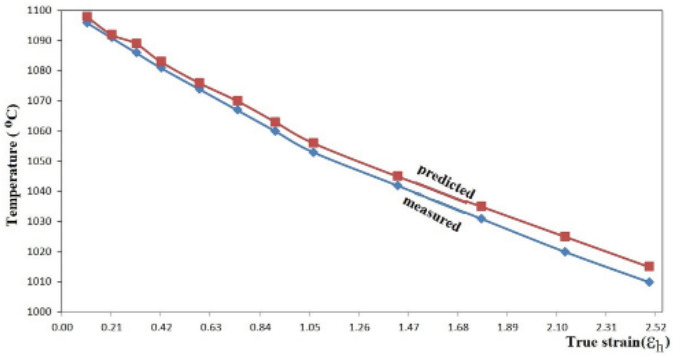

Fig. 13. Comparison of the computed temperature and the measured temperature during the cogging process of X6CrNiTi18-10 steel specimens in flat anvils. Forging ratio of 4.0

The experimental confirmation of the results of the numerical investigations of the effective strain distribution, and also the average grain size after forging in radial-rhombic anvils with an impression angle of $\alpha = 135° \times 135°$, are presented in Figure 14. The strain state has been determined using the coordination grid method. The predicted simulation results compared well with experimental measurements.

5. Conclusions

The conducted research made it possible to determine the local values typical of the strain state, the state of stress, temperature distribution and the parameters of microstructure in the course of the forging of the X6CrNiTi18-10 austenitic steel on flat and shaped anvils. The application of the two-stage process of deformation with the introduction, in the initial phase, of forging on the convex anvils with an angle of 135°, in combination with the final deformation on shaped anvils to obtain the required forging ratio, brought about significant changes to the kinematics of metal flow. That made it possible to attain the effective strain distributions similar to uniform, and also to obtain a homogeneous and fine-crystallite microstructure. On flat anvils, the greatest non-uniformity of the effective strain distribution was obtained, with the adverse condition of stress in the lateral zones of a forging, and also the largest average grain size. The analysis of the results of research indicates the particularly significant influence exerted by the forging ratio upon the values and the effective strain distribution, mean stresses and the parameters of microstructure in the course of multi-stage cogging process.

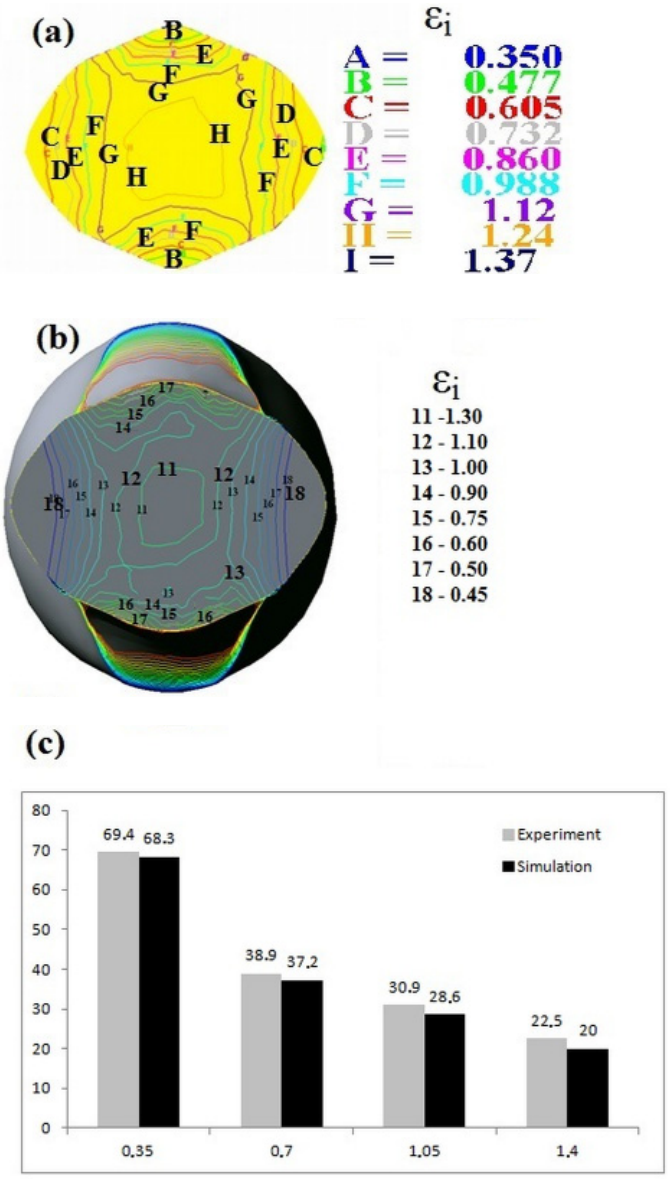

Fig. 14. Comparisons of the theoretical (a) and experimental (b) effective strain (ε_i) distribution on the cross-sectional surfaces of X6CrNiTi18-10 steel specimens deformed in radial-rhombic anvils with an impression angle of $\alpha = 135° \times 135°$ (relative feed $l_w = 0.75$; true strain $\varepsilon_h = 0.70$), (c) comparisons between the experimental and simulated results (average grain sizes in the centre of the specimens deformed in radial-rhombic anvils at different true strain)

REFERENCES

[1] H. Sun, Y. Sun, R. Zhang, M. Wang, R. Tang, Z. Zhou, Study on hot workability and optimization of process parameters of a modified 310 austenitic stainless steel using processing maps, Materials and Design **67**, 165-172 (2015).

[2] H. Sun, Y. Sun, R. Zhang, M. Wang, R. Tang, Z. Zhou, Study on hot workability and optimization of process parameters of a modified 310 austenitic stainless steel using processing maps, Materials and Design **67**, 165-172 (2015).

[3] W. Zhang, S. Sun, D. Zhao, B. Wang, Z. Wang, W. Fu, Hot deformation behavior of a Nb-containing 316 LN stainless steel, Materials and Design **32**, 4173-4179 (2011).

[4] G. Liu, Y. Han, Z. Shi, J. Sun, D. Zou, G. Qiao, Hot deformation and optimization of process parameters of an as-cast 6Mo super-austenitic stainless steel: A study with processing map, Materials and Design **53**, 662-672 (2014).

[5] G.Z. Quan, J.T. Liang, Y.Y. Liu, G.C. Luo, Y. Shi, J. Zhou, Identification of optimal deforming parameters from a large range of strain, strain rate and temperature for 3Cr20Ni10W2 heat-resistant alloy, Materials and Design **52**, 593-601 (2013).

[6] Y. Kim, J. Cho, W. Bae, Efficient forging process to improve the closing effect of the inner void on an ultra-large ingot. Journal of Materials Processing Technology **211**, 1005-1013 (2011).

[7] M. Kukuryk, The influence of technological parameters on the effectiveness of the cogging process, Hutnik – Wiadomości Hutnicze **81**, 646-651 (2014).

[8] N.T. Switzner, C.J. Van Tyne, M.C. Mataya, Effect of forging strain rate and deformation temperature on the mechanical properties of warm-worked 304L stainless steel, Journal of Materials Processing Technology **210**, 998-1007 (2010).

[9] S.K. Choi, M.S. Chun, C.J. Van-Tyne, Y.H. Moon, Optimization of open die forging of round shapes using FEM analysis, Journal of Materials Processing Technology **172**, 88-95 (2006).

[10] J. Brnic, G. Turkalj, M. Canadija, S. Krscanski, M. Brcic, D. Lanc, Deformation behaviour and material properties of austenitic heat--resistant steel X15CrNiSi25-20 subjected to high temperatures, Materials and Design **69**, 219-2239 (2015).

[11] H. Sun, Y. Sun, R. Zhang, M. Wang, R. Tang, Z. Zhou, Hot deformation behavior and microstructural evolution of a modified 310 austenitic steel, Materials and Design **64**, 374-380 (2014).

[12] J. Fluhrer, Deform 3D User's Manual Version 6.0, Scientific Forming Technologies Corporation, Columbus, OH (2006).

[13] M. Kukuryk, Analysis of deformation and microstructural evolution in the hot forging of the Ti-6Al-4V alloy, Archives of Metallurgy and Materials **60**, 1639-1647 (2015).

[14] Y.C. Lin, X.M. Chen, D.X. Wen, M.S. Chen, A physically - based constitutive model for a typical nickel-based superalloy, Computational Materials Science **83**, 282-289 (2014).

[15] G.Z. Quan, A. Mao, G.C. Luo, J.T. Liang, D.S. Wu, J. Zhou, Constitutive modelling for the dynamic recrystallization kinetics of as – extruded 3Cr20Ni10W2 heat- resistant alloy based on stress-strain data, Materials and Design **52**, 98-107 (2013).

[16] Y.C. Lin, M.S. Chen, Numerical simulation and experimental verification of microstructure evolution in a three-dimensional hot upsetting process, Journal of Materials Processing Technology **209**, 4578-4583 (2009).